Electronic Supplementary Information (ESI) for:

Choosing the ideal photoinitiator for free radical photopolymerizations: Predictions based on simulations using established data

Anna Eibel, David E. Fast, and Georg Gescheidt

Institute of Physical and Theoretical Chemistry, Graz University of Technology,
Stremayrgasse 9, 8010 Graz, Austria
E-mail: g.gescheidt-demner@tugraz.at

1. Photoinitiators, LED Light Sources and Measurement of UV-Vis and LFP Spectra

The photoinitiators 2-hydroxy-2-methylpropiophenone (Darocur® 1173, **1**) and diphenyl(2,4,6-trimethylbenzoyl)phosphine oxide (Irgacure® 819, **2**) were obtained from Sigma Aldrich. Diethyldibenzoylgermane (**3**) was kindly provided by Ivoclar Vivadent AG. Tetrabenzoylgermane (**4**) was kindly provided by the research group of Prof. Stueger (Graz University of Technology).

The intensity of the 385 nm LED was measured using a calibrated spectrophotometer (GL Spectis 1.0, GL Optic Lichtmesstechnik GmbH, Weilheim, Germany) equipped with an integrating sphere. The measured power of the LED *P* (in W) can be translated into the spectral photon flux I_0 in mol s^{-1} L^{-1}:[1]

$$I_0 = \frac{\lambda P}{hcN_A V}$$

Here, *λ* is the peak wavelength of the light source (in m), *h* is Planck's constant (h = 6.63·10-34 J·s), *c* is the speed of light in vacuum (c = 299792458 m·s^{-1}), N_A is Avogadro's constant (N_A = 6.02·1023 mol^{-1}), and *V* is the reaction volume in L (in our case, we consider a sample volume of 2 mL).

UV-Vis spectra were recorded on a TIDAS UV-Vis spectrometer (J&M, Germany). Photoinitiator samples were prepared at concentrations of 1 mM in acetonitrile (Sigma Aldrich, ≥ 99.9%). Measurements were performed spectrometer in a fluorescence quartz cuvette (1 cm x 1 cm).

Laser-flash photolysis (LFP) experiments were performed on a LKS80 Laser Flash Photolysis Spectrometer (Applied Photophysics, UK). Samples were excited with the frequency tripled light from a Spitlight Compact 100 (InnoLas, Germany) solid state Nd:YAG laser at 355 nm (~10 mJ/pulse, 8 ns). Rate constants for the quenching of the germyl by oxygen were determined in pseudo-first-order experiments; solutions of compounds **3** and **4** in acetonitrile containing oxygen concentrations in the range of 0.6 mM to 1.6 mM and providing absorbance of ~0.3 at 355 nm were prepared. The decay of the germyl radicals was recorded at the absorption maximum determined from the transient absorption spectra. Exponential fitting of the decay traces obtained at various quencher concentrations yield the pseudo-first order rate constants k_{exp}. The second order oxygen quenching rate constants k_{ox}

---

[1] According to IUPAC, the unit "mol s^{-1} m^{-3}" is the SI unit for the spectral photon flux (photon irradiance), see https://goldbook.iupac.org/html/S/S05821.html.

are obtained from the slope of their linear dependence on the oxygen concentration (see Figure S1).

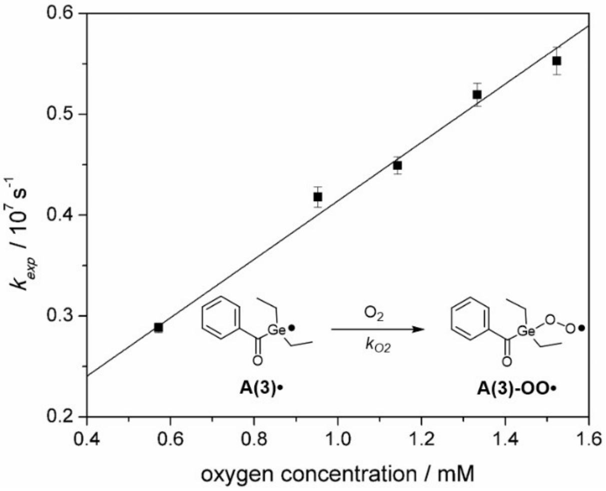

Figure S1. Pseudo-first-order decay rate constant (k_{exp}) of radical **A(3)•** versus oxygen concentration (excitation wavelength: 355 nm, monitoring wavelength: 480 nm). The slope of the curve yields $k_{ox} = 2.90 \pm 0.14 \cdot 10^9$ $Lmol^{-1}s^{-1}$.

2. Simulations of Radical Generation at Various Wavelengths and Light Intensities

Figures S2 and S3 present simulations of the radical generation upon irradiation of **1-4** upon irradiation at 350 nm and 450 nm. For both wavelengths, simulations were performed for the same photon flux as for irradiation at 385 nm ($I_0 = 2 \times 10^{-5}$ mol $L^{-1}s^{-1}$). At 350 nm, radical generation is most efficient for bisacylphosphane oxide **2**, while bisacylgermane **3** shows poor efficiency, which is consistent with the low extinction coefficient of **3** at 350 nm (compare Figure 1 in the main text). This situation is turned upon irradiation at 450 nm, where initiator **3** shows the best performance (**3** > **4** > **2** >> **1**, see Figure S3). When comparing **3** and **4** at 450 nm, the extinction coefficients are very similar (227 and 214 L mol^{-1} cm^{-1}, respectively), yet the higher quantum yield of **3** results in significantly faster generation of the primary radicals **A•** and **B•** when compared to **4**.

Figure S4 demonstrates the effect of increasing the spectral photon flux I_0. The radical generation is simulated at 350 nm for a 10 times higher photon flux when compared to Figure S1 ($I_0 = 2 \times 10^{-4}$ mol $L^{-1}s^{-1}$). As evident from equation 1 (main text), the radical generation occurs at a 10 times faster time scale in this case.

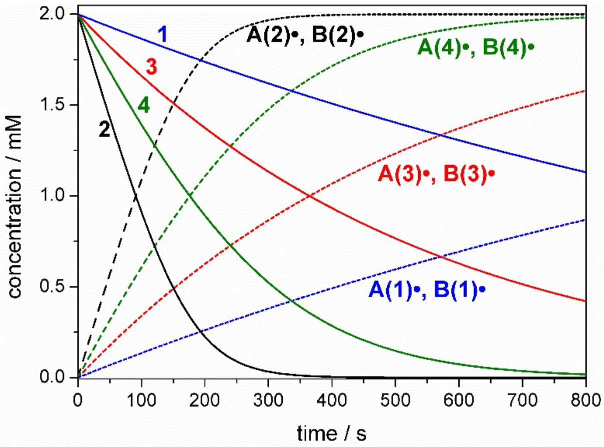

Figure S2. Simulated concentration versus time plots for the parent photoinitiators **1-4** and the primary radicals **A(1-4)•** and **B(1-4)•**. Chosen conditions: irradiation at 350 nm ($I_0 = 2 \cdot 10^{-5}$ mol L^{-1} s^{-1}), photoinitiator concentrations: 2 mM.

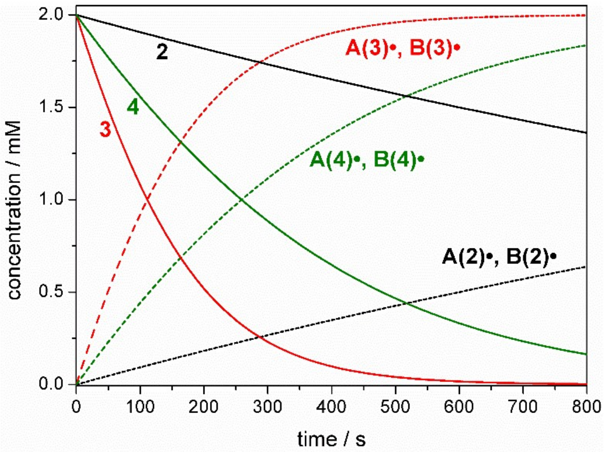

Figure S3. Simulated concentration versus time plots for the parent photoinitiators **2-4** and the primary radicals **A(2-4)•** and **B(2-4)•**. Chosen conditions: irradiation at 450 nm ($I_0 = 2 \cdot 10^{-5}$ mol L^{-1} s^{-1}), photoinitiator concentrations: 2 mM. Compound **1** is not included in this simulation since it does not absorb light at 450 nm.

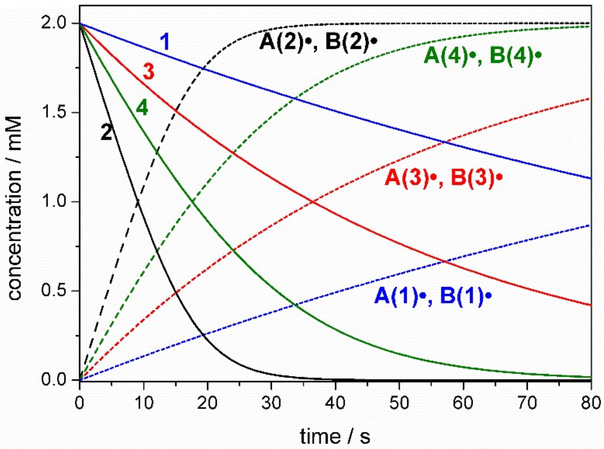

Figure S4. Simulated concentration versus time plots for the parent photoinitiators **1-4** and the primary radicals **A(1-4)•** and **B(1-4)•** for irradiation with a higher photon flux. Chosen conditions: irradiation at 350 nm ($I_0 = 2 \cdot 10^{-4}$ mol L^{-1} s^{-1}), photoinitiator concentrations: 2 mM.

3. Simulations of Radical Generation and Subsequent Addition to the Monomer

Figures S5-S7 present simulations of initiation reaction for photoinitiators **1**, **2** and **4** in bulk butyl acrylate. The simulations for compounds **2** and **4** were performed for irradiation (low photon flux I_0) at 385 nm, while 320 nm were chosen for **1**, a wavelength which matches better with the UV-Vis spectrum of this compound. Figures S5-S7 a) show simulations using the experimental values of Φ, ε and k_{add}, whereas in the Figures b)-d) one of these parameters has been reduced by 50 % to show their impact on the product radical generation rate. Notably, in all cases, the highest impact on the radical generation rate is observed upon reduction of the quantum yield, followed by the extinction coefficient. As discussed in the main text, a change of the addition rate constants is barely noticeable in the simulations.

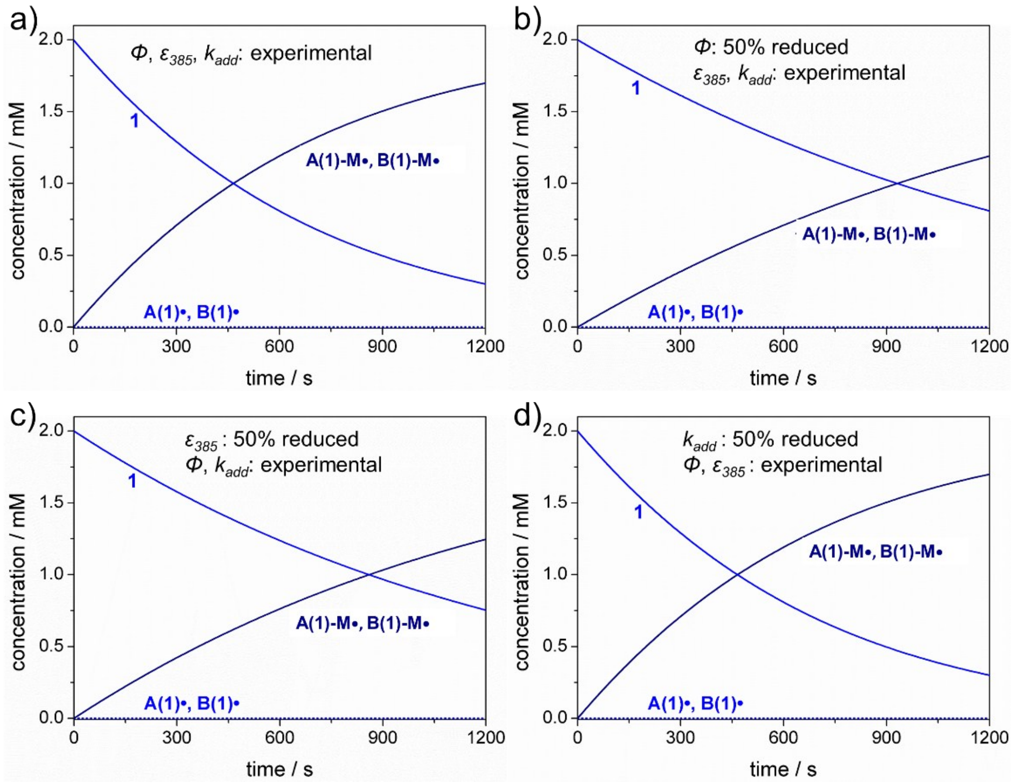

Figure S5. Simulation of the initiation reaction (radical generation followed by monomer addition) for compound **1** in bulk butyl acrylate at 320 nm (I_0 = 2x10^{-5} mol L^{-1}s^{-1}, concentrations: 2 mM **1**, 7 M butyl acrylate, **M**). Concentration versus time plots for a) Φ = 0.38, ε_{320} = 100 L mol^{-1} cm^{-1}, $k_{add,\mathbf{A(1)\bullet}}$ = 1.3 x 10^{7} L mol^{-1} s^{-1}, $k_{add,\mathbf{B(1)\bullet}}$ = 2.7 x 10^{5} L mol^{-1} s^{-1}; b) Φ = 0.195, ε_{320} = 100 L mol^{-1} cm^{-1}, $k_{add,\mathbf{A(1)\bullet}}$ = 1.3 x 10^{7} L mol^{-1} s^{-1}, $k_{add,\mathbf{B(1)\bullet}}$ = 2.7 x 10^{5} L mol^{-1} s^{-1}; c) Φ = 0.38, ε_{320} = 50 L mol^{-1} cm^{-1}, $k_{add,\mathbf{A(1)\bullet}}$ = 1.3 x 10^{7} L mol^{-1} s^{-1}, $k_{add,\mathbf{B(1)\bullet}}$ = 2.7 x 10^{5} L mol^{-1}s^{-1}; d) Φ = 0.38, ε_{320} = 100 L mol^{-1} cm^{-1}, $k_{add,\mathbf{A(1)\bullet}}$ = 6.5 x 10^{6} L mol^{-1} s^{-1}, $k_{add,\mathbf{B(1)\bullet}}$ = 1.35 x 10^{5} L mol^{-1} s^{-1}.

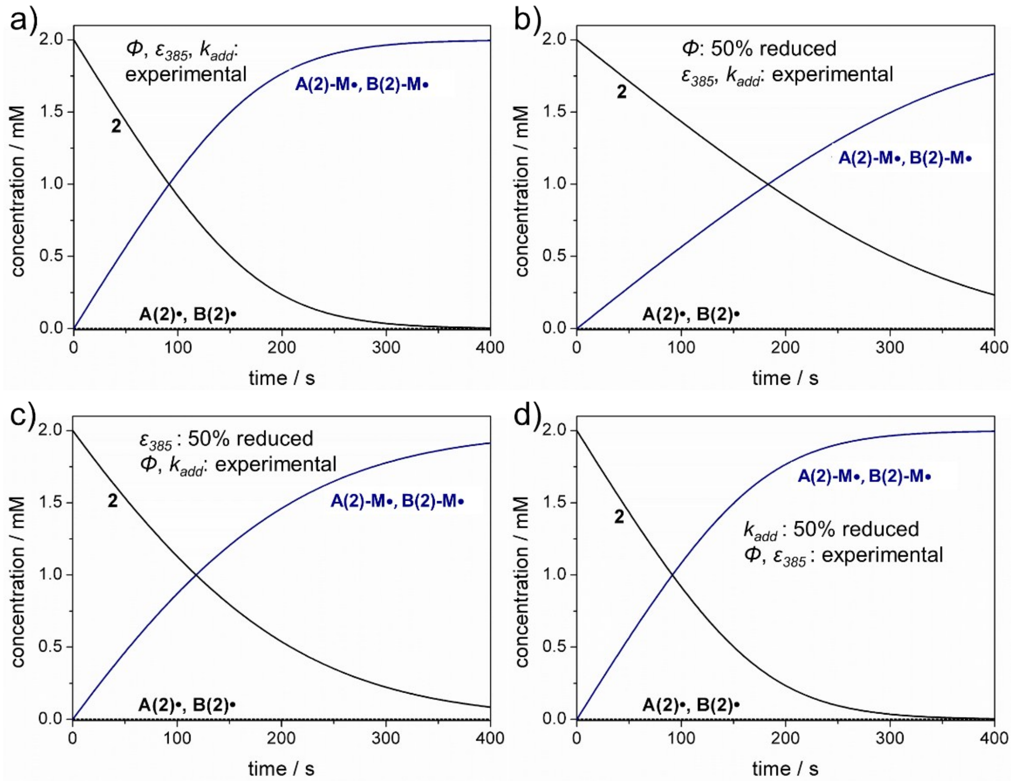

Figure S6. Simulation of the initiation reaction (radical generation followed by monomer addition) for compound **2** in bulk butyl acrylate at 385 nm (I_0 = 2x10^{-5} mol L^{-1}s^{-1}, concentrations: 2 mM **2**, 7 M butyl acrylate, **M**). Concentration versus time plots for a) Φ = 0.60, ε_{385} = 740 L mol^{-1} cm^{-1}, $k_{add,\mathbf{A(2)\bullet}}$ = 1.1 x 10^7 L mol^{-1} s^{-1}, $k_{add,\mathbf{B(2)\bullet}}$ = 1.8 x 10^5 L mol^{-1} s^{-1}; b) Φ = 0.30, ε_{385} = 740 L mol^{-1} cm^{-1}, $k_{add,\mathbf{A(2)\bullet}}$ = 1.1 x 10^7 L mol^{-1} s^{-1}, $k_{add,\mathbf{B(2)\bullet}}$ = 1.8 x 10^5 L mol^{-1} s^{-1}; c) Φ = 0.60, ε_{385} = 370 L mol^{-1} cm^{-1}, $k_{add,\mathbf{A(2)\bullet}}$ = 1.1 x 10^7 L mol^{-1} s^{-1}, $k_{add,\mathbf{B(2)\bullet}}$ = 1.8 x 10^5 L mol^{-1}s^{-1}; d) Φ = 0.60, ε_{385} = 740 L mol^{-1} cm^{-1}, $k_{add,\mathbf{A(2)\bullet}}$ = 5.50 x 10^6 L mol^{-1} s^{-1}, $k_{add,\mathbf{B(2)\bullet}}$ = 9 x 10^4 L mol^{-1} s^{-1}.

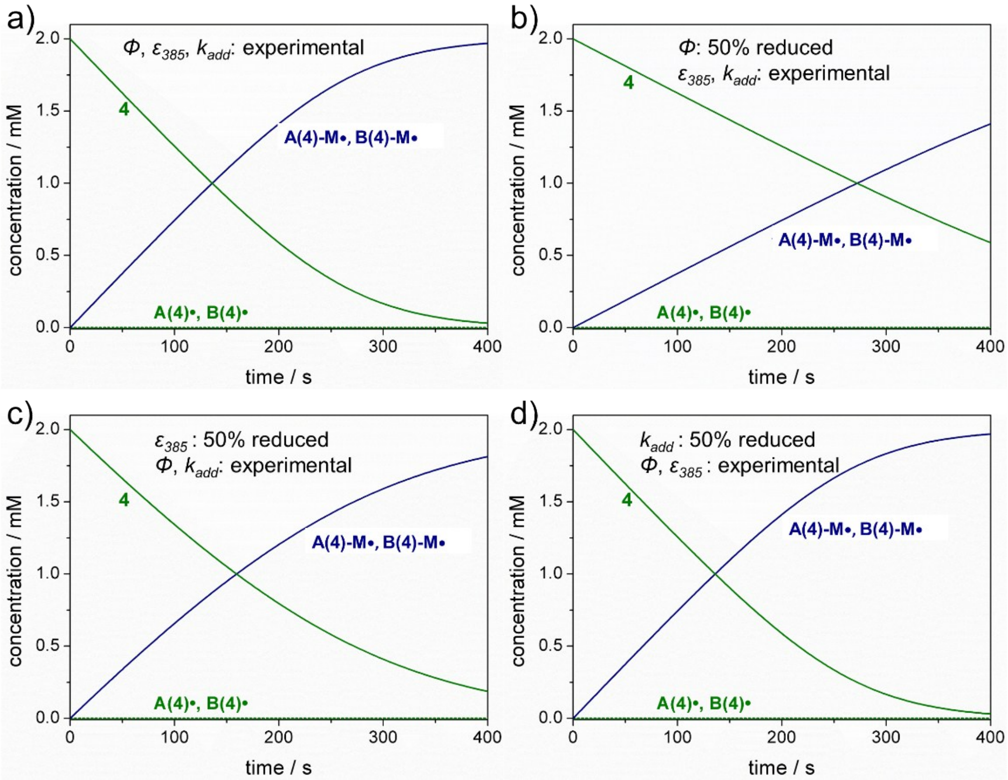

Figure S7. Simulation of the initiation reaction (radical generation followed by monomer addition) for compound **4** in bulk butyl acrylate at 385 nm (I_0 = 2x10^{-5} mol L^{-1}s^{-1}, concentrations: 2 mM **4**, 7 M butyl acrylate, **M**). Concentration versus time plots for a) Φ = 0.38, ε_{385} = 1060 L mol^{-1} cm^{-1}, $k_{add},_{\mathbf{A(2)\bullet}}$ = 5.9 x 10^{7} L mol^{-1} s^{-1}, $k_{add},_{\mathbf{B(2)\bullet}}$ = 2.7 x 10^{5} L mol^{-1} s^{-1}; b) Φ = 0.19, ε_{385} = 1060 L mol^{-1} cm^{-1}, $k_{add},_{\mathbf{A(2)\bullet}}$ = 5.9 x 10^{7} L mol^{-1} s^{-1}, $k_{add},_{\mathbf{B(2)\bullet}}$ = 2.7 x 10^{5} L mol^{-1}s^{-1}; c) Φ = 0.38, ε_{385} = 530 L mol^{-1} cm^{-1}, $k_{add},_{\mathbf{A(2)\bullet}}$ = 5.9 x 10^{7} L mol^{-1} s^{-1}, $k_{add},_{\mathbf{B(2)\bullet}}$ = 2.7 x 10^{5} L mol^{-1}s^{-1}; d) Φ = 0.38, ε_{385} = 1060 L mol^{-1} cm^{-1}, $k_{add},_{\mathbf{A(2)\bullet}}$ = 2.95 x 10^{7} L mol^{-1} s^{-1}, $k_{add},_{\mathbf{B(2)\bullet}}$ = 1.35 x 10^{5} L mol^{-1} s^{-1}.

Figures S8-S10 present simulations of initiation reaction for photoinitiators **1**, **2** and **4** at high photon flux I_0 for bulk and solution polymerizations. The addition rate constants become relevant under these conditions, leading to a higher initiation efficiency for the more reactive radicals **A(1, 2, 4)•** when compared to the less reactive radicals **B(1, 2, 4)•**. The effects of the different addition rate constants are more pronounced in solution polymerization when compared to bulk polymerizations (compare the main text).

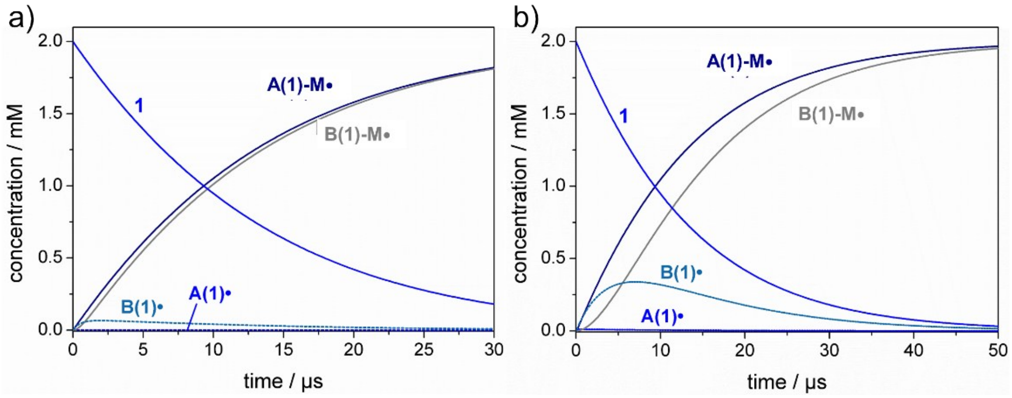

Figure S8. Simulation of the initiation reaction (radical generation followed by monomer addition) for compound **1** for photolysis with a hypothetical high power 320 nm lamp (I_0 = 1000 mol L^{-1} s^{-1}): a) bulk polymerization (7 M butyl acrylate, **M**), b) solution polymerization (1 M butyl acrylate, **M**).

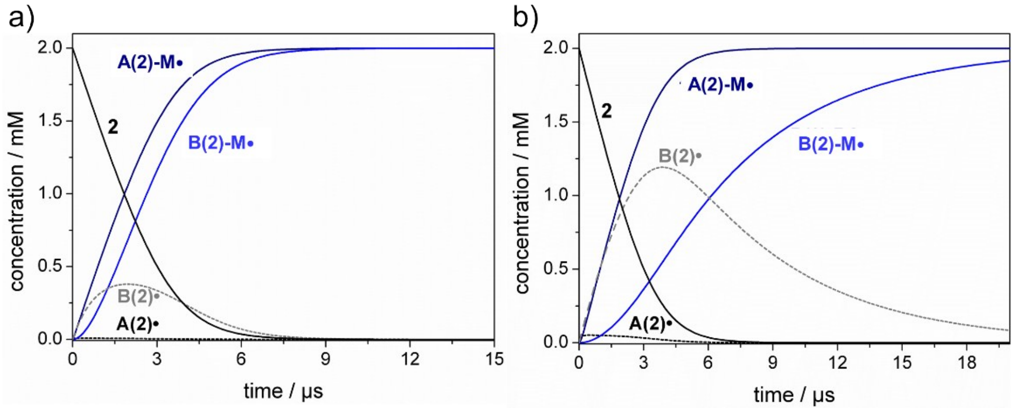

Figure S9. Simulation of the initiation reaction (radical generation followed by monomer addition) for compound **2** for photolysis with a hypothetical high power 385 nm lamp (I_0 = 1000 mol L^{-1} s^{-1}): a) bulk polymerization (7 M butyl acrylate, **M**), b) solution polymerization (1 M butyl acrylate, **M**).

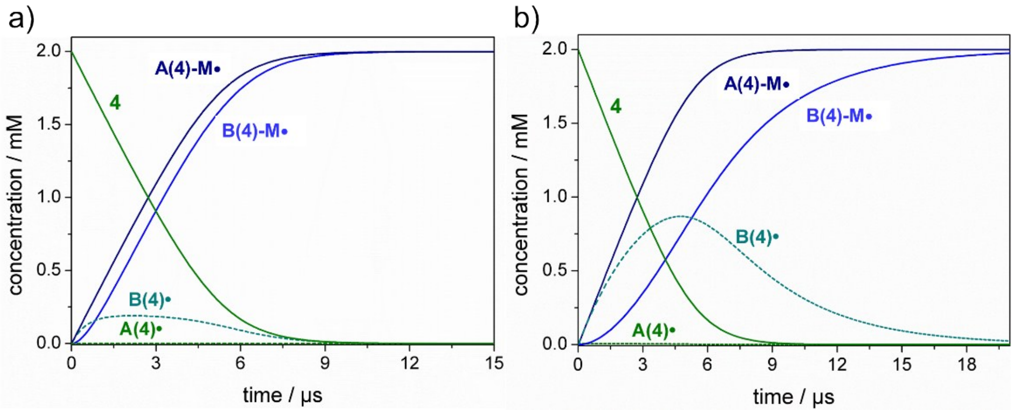

Figure S10. Simulation of the initiation reaction (radical generation followed by monomer addition) for compound **4** for photolysis with a hypothetical high power 385 nm lamp (I_0 = 1000 mol L^{-1} s^{-1}): a) bulk polymerization (7 M butyl acrylate, **M**), b) solution polymerization (1 M butyl acrylate, **M**).

Figure S11 presents simulations of initiation reaction for photoinitiator **3** for both irreversible and reversible addition of the primary radicals **A•** and **B•** to butyl acrylate **M**. For the reverse rate constant, a value corresponding to 20% of the forward reaction was chosen (see the main text). Simulations are performed for bulk polymerization under both low and high power illumination (Figure S11).

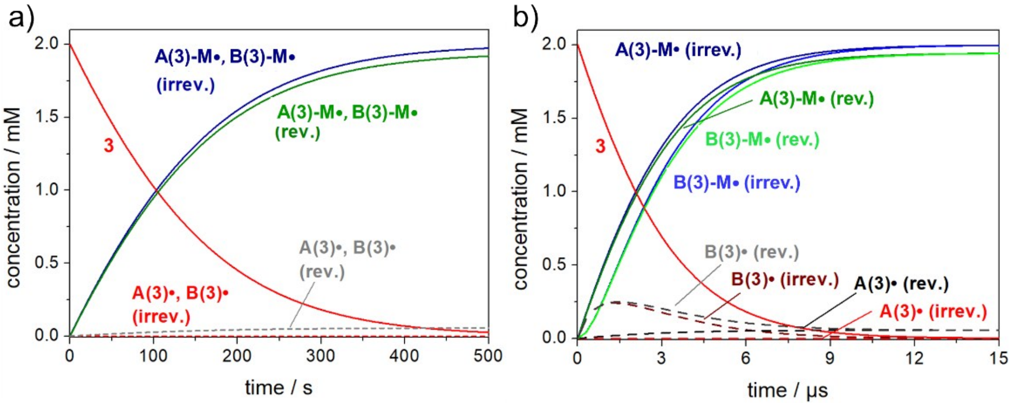

Figure S11. Simulation of the initiation reaction (radical generation followed by monomer addition) for compound **3** in bulk butyl acrylate under reversible conditions ($k_{add,\mathbf{A\bullet}}$ = 2.6 x 10^8 L $mol^{-1}s^{-1}$, $k_{add,\mathbf{A\bullet}\ back}$ =5.2 x 10^7 L $mol^{-1}s^{-1}$, $k_{add,\mathbf{B\bullet}}$ = 2.7 x 10^5 L mol^{-1} s^{-1}, $k_{add,\mathbf{B\bullet}\ back}$ =5.4 x 10^4 L $mol^{-1}s^{-1}$): a) Photolysis with a low power 385 nm LED (I_0 = 2 x 10^{-5} mol L^{-1} s^{-1}), b) Photolysis with a hypothetical high power 385 nm lamp (I_0 = 1000 mol L^{-1} s^{-1}). Products formed by assuming an irreversible addition of the primary radicals **A•** and **B•** to butyl acrylate **M** are marked with (**irrev**.), and products formed by assuming reversible addition are marked with (**rev**.).

Figure S12 presents simulations of initiation reaction of photoinitiator **3** for the (irreversible) addition of the primary radicals **A(3)•** and **B(3)•** to butyl acrylate **M**, considering the recombination of two primary radicals as a side reaction. These recombination reaction lead to the products **A(3)-B(3)** (equivalent to the parent photoinitiator **3**, which can subsequently be photolyzed again), as well as the products **A(3)-A(3)** and **B(3)-B(3)** (see Scheme S1). In the simulations presented in Figure S12, we assume diffusion controlled recombination (recombination rate constant $k_r \sim 10^9$ L $mol^{-1}s^{-1}$).

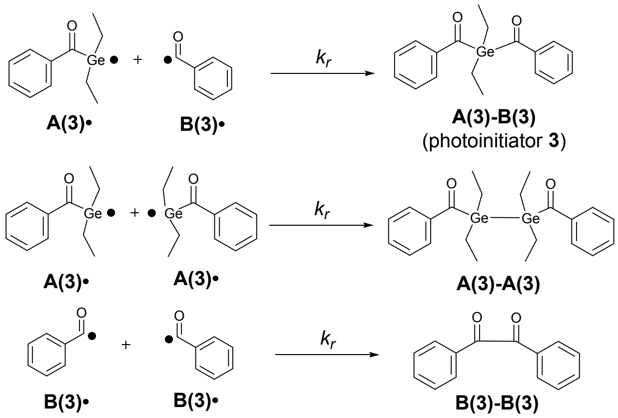

Scheme S1. Recombination reactions of primary radicals **A(3)•** and **B(3)•** as a side reaction to monomer addition. Recombination of the radicals **A(3)•** and **B(3)•** leads to the regeneration of the parent photoinitiator **3**, which can undergo a subsequent bond cleavage.

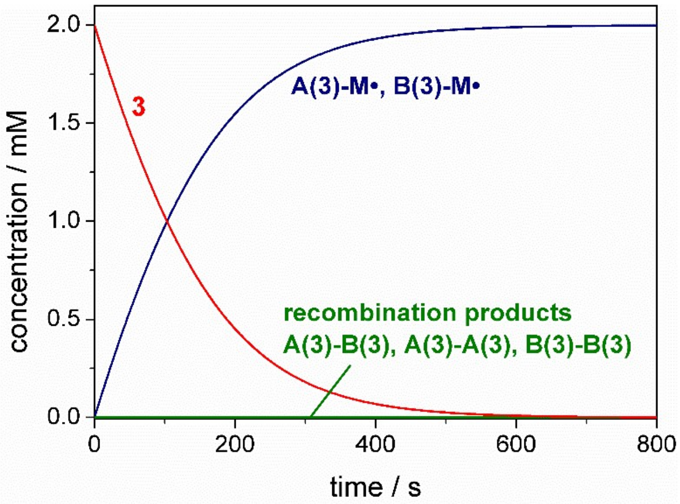

Figure S12. Simulation of the initiation reaction (radical generation followed by monomer addition) for compound **3** for photolysis with a 385 nm LED (I_0 = 2x10^{-5} mol $L^{-1}s^{-1}$) in bulk butyl acrylate (7 M butyl acrylate, **M**). Recombination of primary radicals is considered as a side reaction competing with monomer addition.

In Figure S13, the recombination of the primary radicals with a previously formed addition radical **A(3)-M•** or **B(3)-M•** is considered as a side reaction (see Scheme S2). Bimolecular recombination rate constants k_t are reported to be in the order of 10^6 - 10^8 L mol^{-1} s^{-1} in the literature (see references 12, 34 and 53 in the main text). Even when assuming a termination rate constant of 10^8 L mol^{-1} s^{-1} (upper limit of values reported in the literature), the termination products **A(3)-M-A(3)**, **A(3)-M-B(3)**, **B(3)-M-A(3)** and **B(3)-M-B(3)** are formed to a minor extent (see Figure S13).

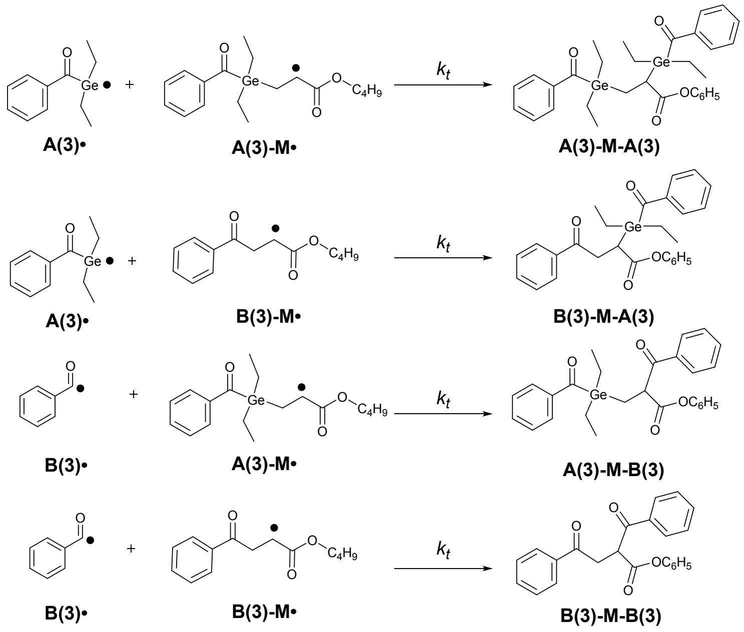

Scheme S2. Termination reaction via recombination of primary radicals **A(3)•** and **B(3)•** with a previously formed addition radical **A(3)-M•** or **B(3)-M•**.

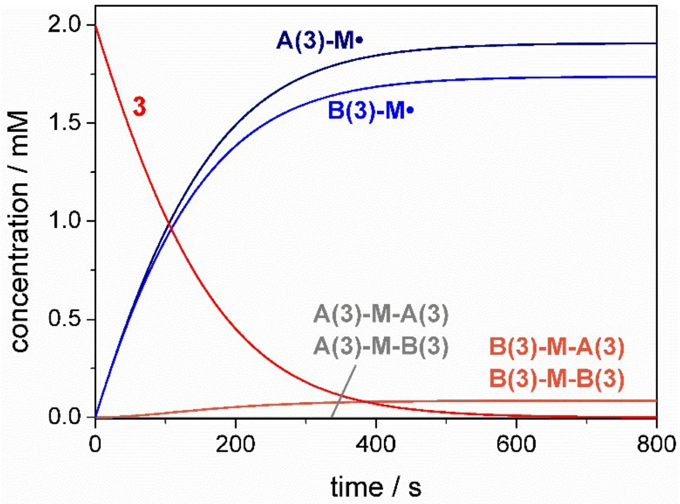

Figure S13. Simulation of the initiation reaction (radical generation followed by monomer addition) for compound **3** for photolysis with a 385 nm LED (I_0 = 2x10^{-5} mol L^{-1}s^{-1}) in bulk butyl acrylate (7 M butyl acrylate, **M**). Recombination of primary radicals with an addition radical **A(3)-M•** or **B(3)-M•** is considered as a side reaction.

4. Simulations of Radical-to-Monomer Addition in Presence of Oxygen

Figures S14-S16 present simulations of the initiation reaction for photoinitiators **1**, **2** and **4** in presence of oxygen for bulk and solution polymerizations upon irradiation with low power LED light (320 nm in case of compound **1** and 385 nm in case of compounds **2** and **4**). As observed for compound **3** (see Figure 4 in the main text), the benzoyl radicals **B(1,2,4)•** of the initiators **1**, **2** and **4** are significantly quenched by oxygen due to the low monomer addition rate constants of these radicals. In case **1**, **2** and **4**, also the ketyl, phosphanoyl and germyl radicals **A(1,2,4)•** undergo oxygen quenching to a significant extend, especially in solution polymerization. This is due to the lower monomer addition rate constants of **A(1,2,4)•** when compared to **A(3)•** (see Table 2 in the main text). In case of PIs **1** and **2**, the main product radical formed at the highest rate in solution polymerization is the **B-OO•** peroxyl radical instead of the **A-BA•** addition radical.

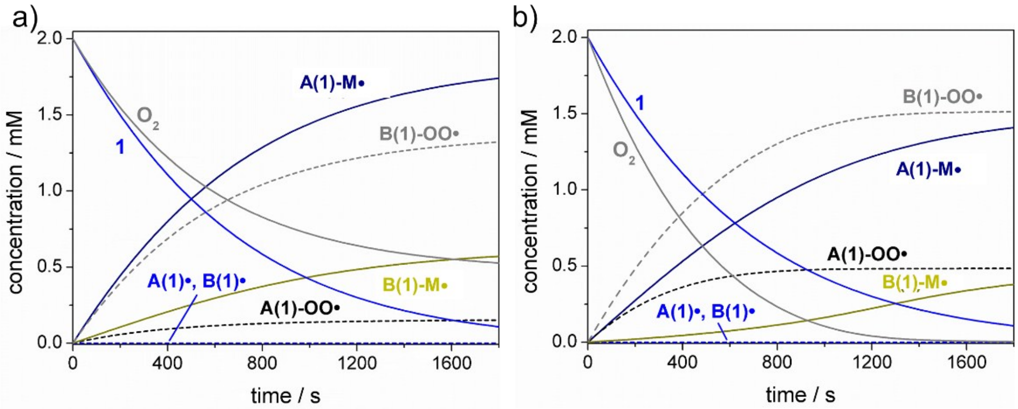

Figure S14. Simulation of the initiation reaction for compound **1** in air-saturated butyl acrylate (320 nm low power LED, I_0 = 2 x 10^{-5} mol L^{-1} s^{-1}, concentrations: 2 mM **1**, 2 mM O_2): a) concentration versus time plot for bulk polymerization (7 M butyl acrylate, **M**); b) concentration versus time plot for solution polymerization (1 M butyl acrylate, **M**).

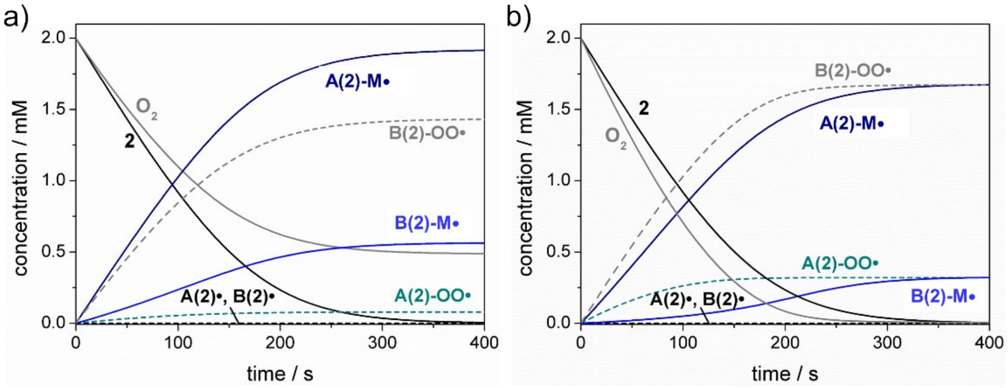

Figure S15. Simulation of the initiation reaction for compound **2** in air-saturated butyl acrylate (385 nm low power LED, I_0 = 2 x 10^{-5} mol L^{-1} s^{-1}, concentrations: 2 mM **2**, 2 mM O_2): a) concentration versus time plot for bulk polymerization (7 M butyl acrylate, **M**); b) concentration versus time plot for solution polymerization (1 M butyl acrylate, **M**).

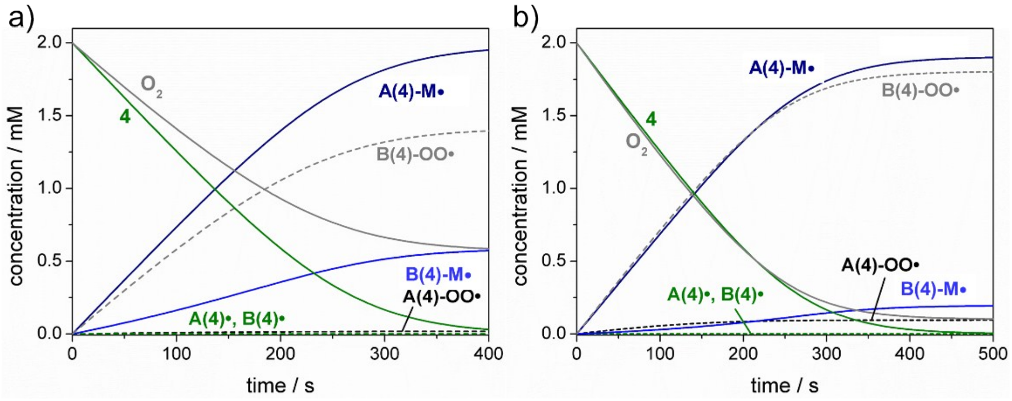

Figure S16. Simulation of the first initiation reaction for compound **4** in air-saturated butyl acrylate (385 nm low power LED, I_0 = 2 x 10^{-5} mol L^{-1} s^{-1}, concentrations: 2 mM **4**, 2 mM O_2): a) concentration versus time plot for bulk polymerization (7 M butyl acrylate, **M**); b) concentration versus time plot for solution polymerization (1 M butyl acrylate, **M**).

5. Detailed Kinetic Model

Table S1 summarizes the reactions considered in our model, together with the kinetic rate laws.

Table S1. Reactions included in the model and the corresponding rate laws (*R*: reaction rates, *k*: rate constants, *Φ*: quantum yield, I_0: spectral photon flux, *ε*: extinction coefficient).

	Equation	**Rate Law**
Radical Generation	$\mathrm{PI} \xrightarrow[\Phi]{h\nu} \mathrm{A}\bullet + \mathrm{B}\bullet$	$R_i = qy \cdot pf \cdot (1 - 10^{-\mathrm{ext}\cdot[\mathrm{P}I]\cdot d})$
Monomer Addition	$\mathrm{A}\bullet + \mathrm{M} \xrightarrow{k_{add}} \mathrm{AM}\bullet$	$R_{add} = k_{add}\,[A\,\bullet][M]$
	$\mathrm{B}\bullet + \mathrm{M} \xrightarrow{k_{add}} \mathrm{BM}\bullet$	$R_{add} = k_{add}\,[B\,\bullet][M]$
O_2 Quenching	$\mathrm{A}\bullet + \mathrm{O_2} \xrightarrow{k_{ox}} \mathrm{AOO}\bullet$	$R_{ox} = k_{ox}\,[A\,\bullet][O_2]$
	$\mathrm{B}\bullet + \mathrm{O_2} \xrightarrow{k_{ox}} \mathrm{BOO}\bullet$	$R_{ox} = k_{ox}\,[B\,\bullet][O_2]$
Recombination	$\mathrm{A}\bullet + \mathrm{B}\bullet \xrightarrow{k_r} \mathrm{A\text{-}B}$	$R_r = k_r\,[A\,\bullet][B\,\bullet]$
	$\mathrm{A}\bullet + \mathrm{A}\bullet \xrightarrow{k_r} \mathrm{A\text{-}A}$	$R_r = k_r\,[A\,\bullet][A\,\bullet]$
	$\mathrm{B}\bullet + \mathrm{B}\bullet \xrightarrow{k_r} \mathrm{B\text{-}B}$	$R_r = k_r\,[B\,\bullet][B\,\bullet]$
Termination	$\mathrm{A}\bullet + \mathrm{AM}\bullet \xrightarrow{k_t} \mathrm{A\text{-}M\text{-}A}$	$R_t = k_t\,[A\,\bullet][AM\,\bullet]$
	$\mathrm{A}\bullet + \mathrm{BM}\bullet \xrightarrow{k_t} \mathrm{A\text{-}M\text{-}B}$	$R_t = k_t\,[A\,\bullet][BM\,\bullet]$
	$\mathrm{B}\bullet + \mathrm{AM}\bullet \xrightarrow{k_t} \mathrm{B\text{-}M\text{-}A}$	$R_t = k_t\,[B\,\bullet][AM\,\bullet]$
	$\mathrm{B}\bullet + \mathrm{BM}\bullet \xrightarrow{k_t} \mathrm{B\text{-}M\text{-}B}$	$R_t = k_t\,[B\,\bullet][BM\,\bullet]$

Figures S17-S20 show screenshots of our simulation program designed with the public-domain software COPASI (see reference 37 in the main text).

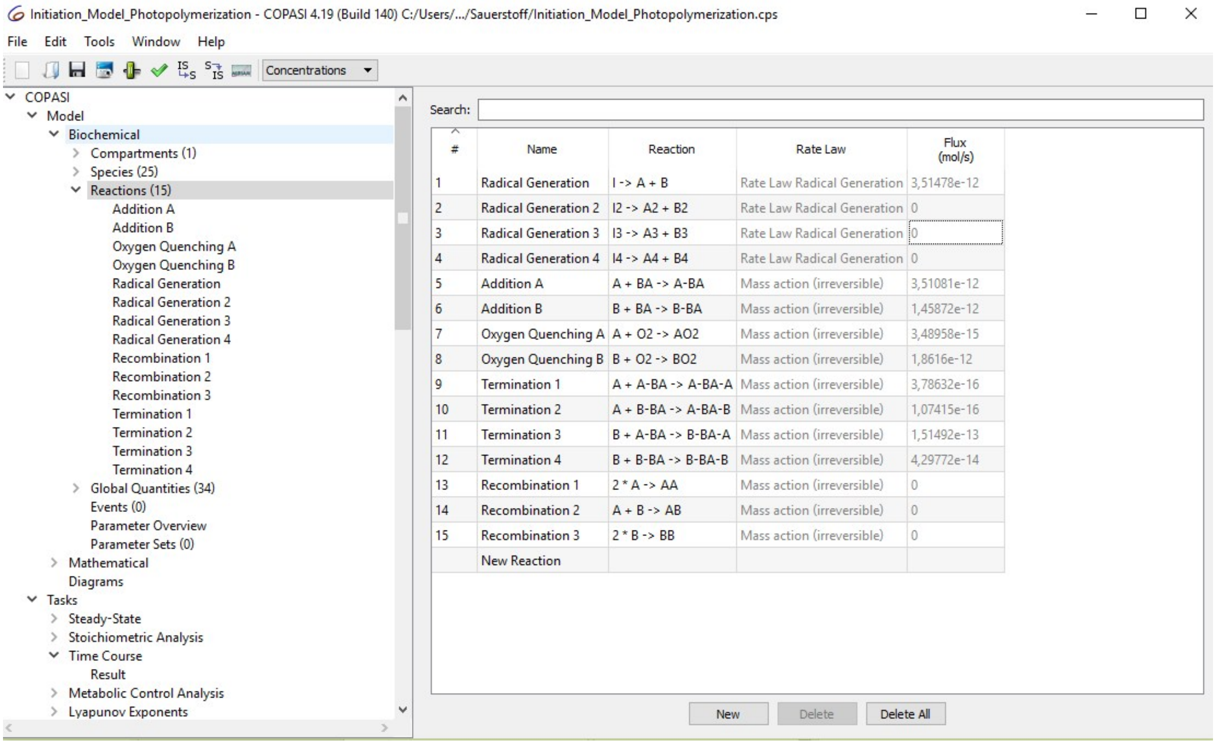

#	Name	Reaction	Rate Law	Flux (mol/s)
1	Radical Generation	I -> A + B	Rate Law Radical Generation	3,51478e-12
2	Radical Generation 2	I2 -> A2 + B2	Rate Law Radical Generation	0
3	Radical Generation 3	I3 -> A3 + B3	Rate Law Radical Generation	0
4	Radical Generation 4	I4 -> A4 + B4	Rate Law Radical Generation	0
5	Addition A	A + BA -> A-BA	Mass action (irreversible)	3,51081e-12
6	Addition B	B + BA -> B-BA	Mass action (irreversible)	1,45872e-12
7	Oxygen Quenching A	A + O2 -> AO2	Mass action (irreversible)	3,48958e-15
8	Oxygen Quenching B	B + O2 -> BO2	Mass action (irreversible)	1,8616e-12
9	Termination 1	A + A-BA -> A-BA-A	Mass action (irreversible)	3,78632e-16
10	Termination 2	A + B-BA -> A-BA-B	Mass action (irreversible)	1,07415e-16
11	Termination 3	B + A-BA -> B-BA-A	Mass action (irreversible)	1,51492e-13
12	Termination 4	B + B-BA -> B-BA-B	Mass action (irreversible)	4,29772e-14
13	Recombination 1	2 * A -> AA	Mass action (irreversible)	0
14	Recombination 2	A + B -> AB	Mass action (irreversible)	0
15	Recombination 3	2 * B -> BB	Mass action (irreversible)	0
	New Reaction			

Figure S17. Screenshot of the reactions considered in the simulation program (BA: butyl acrylate).

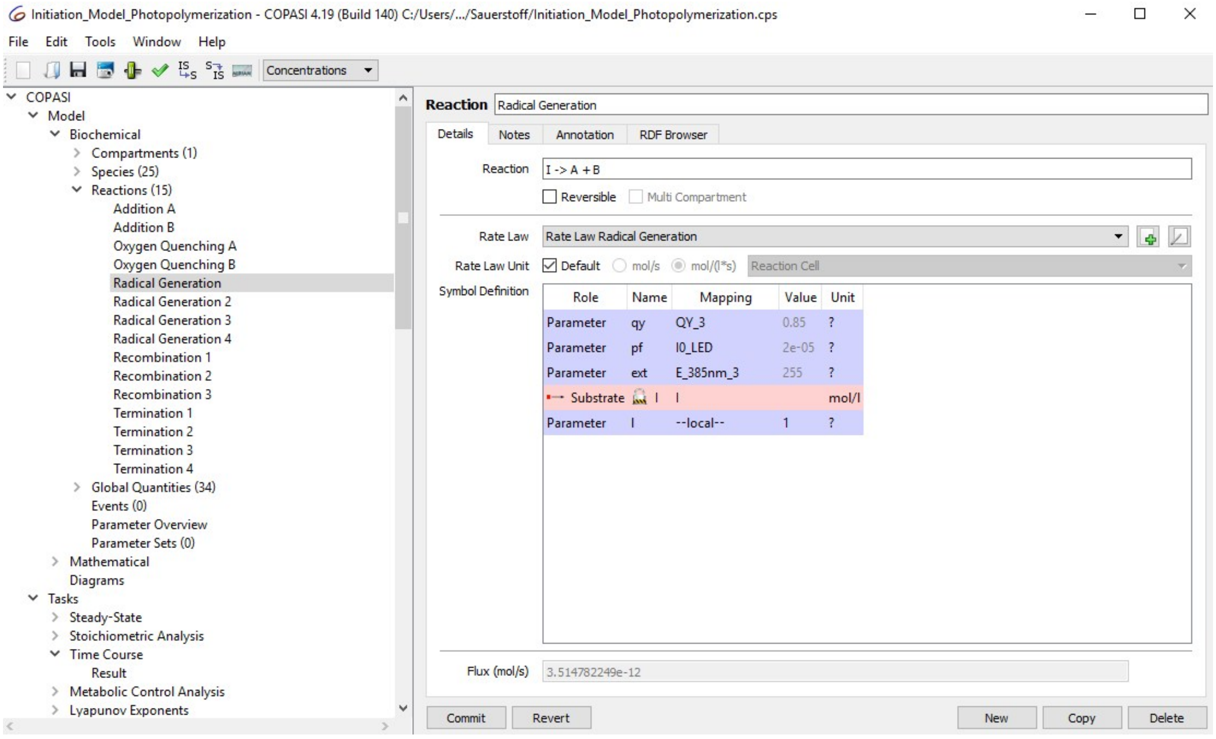

Reaction: Radical Generation

Reaction: I -> A + B

☐ Reversible ☐ Multi Compartment

Rate Law: Rate Law Radical Generation

Rate Law Unit: ☑ Default ○ mol/s ● mol/(l*s) Reaction Cell

Symbol Definition

Role	Name	Mapping	Value	Unit
Parameter	qy	QY_3	0.85	?
Parameter	pf	I0_LED	2e-05	?
Parameter	ext	E_385nm_3	255	?
Substrate	I	I		mol/l
Parameter	I	--local--	1	?

Flux (mol/s): 3.514782249e-12

Figure S18. Screenshot of the parameters defined for the radical generation reaction with compound **3** (qy: quantum yield, pf: spectral photon flux (I_0), ext: extinction coefficient).

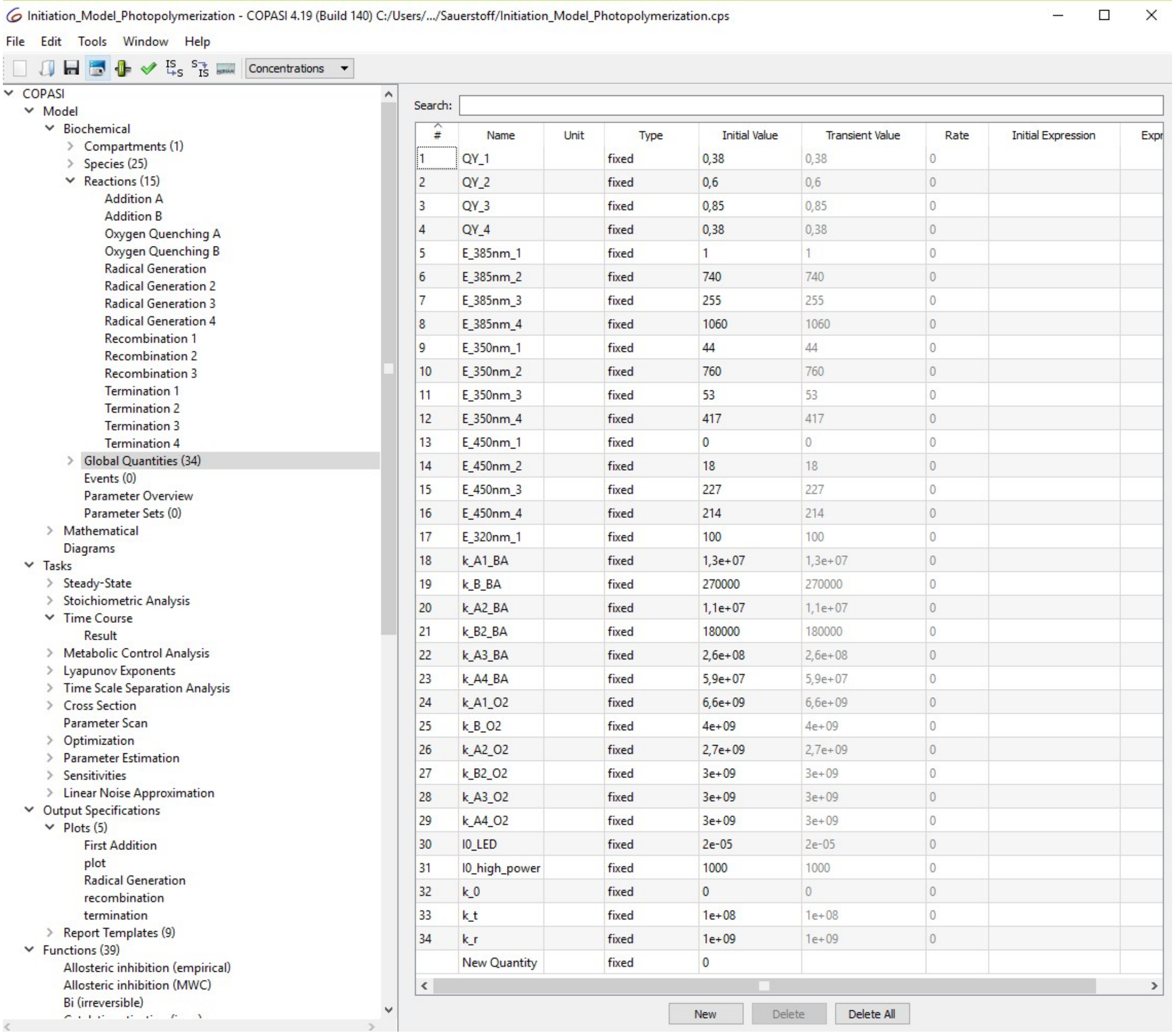

#	Name	Unit	Type	Initial Value	Transient Value	Rate	Initial Expression	Expr
1	QY_1		fixed	0,38	0,38	0		
2	QY_2		fixed	0,6	0,6	0		
3	QY_3		fixed	0,85	0,85	0		
4	QY_4		fixed	0,38	0,38	0		
5	E_385nm_1		fixed	1	1	0		
6	E_385nm_2		fixed	740	740	0		
7	E_385nm_3		fixed	255	255	0		
8	E_385nm_4		fixed	1060	1060	0		
9	E_350nm_1		fixed	44	44	0		
10	E_350nm_2		fixed	760	760	0		
11	E_350nm_3		fixed	53	53	0		
12	E_350nm_4		fixed	417	417	0		
13	E_450nm_1		fixed	0	0	0		
14	E_450nm_2		fixed	18	18	0		
15	E_450nm_3		fixed	227	227	0		
16	E_450nm_4		fixed	214	214	0		
17	E_320nm_1		fixed	100	100	0		
18	k_A1_BA		fixed	1,3e+07	1,3e+07	0		
19	k_B_BA		fixed	270000	270000	0		
20	k_A2_BA		fixed	1,1e+07	1,1e+07	0		
21	k_B2_BA		fixed	180000	180000	0		
22	k_A3_BA		fixed	2,6e+08	2,6e+08	0		
23	k_A4_BA		fixed	5,9e+07	5,9e+07	0		
24	k_A1_O2		fixed	6,6e+09	6,6e+09	0		
25	k_B_O2		fixed	4e+09	4e+09	0		
26	k_A2_O2		fixed	2,7e+09	2,7e+09	0		
27	k_B2_O2		fixed	3e+09	3e+09	0		
28	k_A3_O2		fixed	3e+09	3e+09	0		
29	k_A4_O2		fixed	3e+09	3e+09	0		
30	I0_LED		fixed	2e-05	2e-05	0		
31	I0_high_power		fixed	1000	1000	0		
32	k_0		fixed	0	0	0		
33	k_t		fixed	1e+08	1e+08	0		
34	k_r		fixed	1e+09	1e+09	0		
	New Quantity		fixed	0				

Figure S19. Screen shot of “global quantities” programmed into the model, including quantum yields (QY), extinction coefficients (E), addition rate constants (k) and light intensities (I0), BA: butyl acrylate.

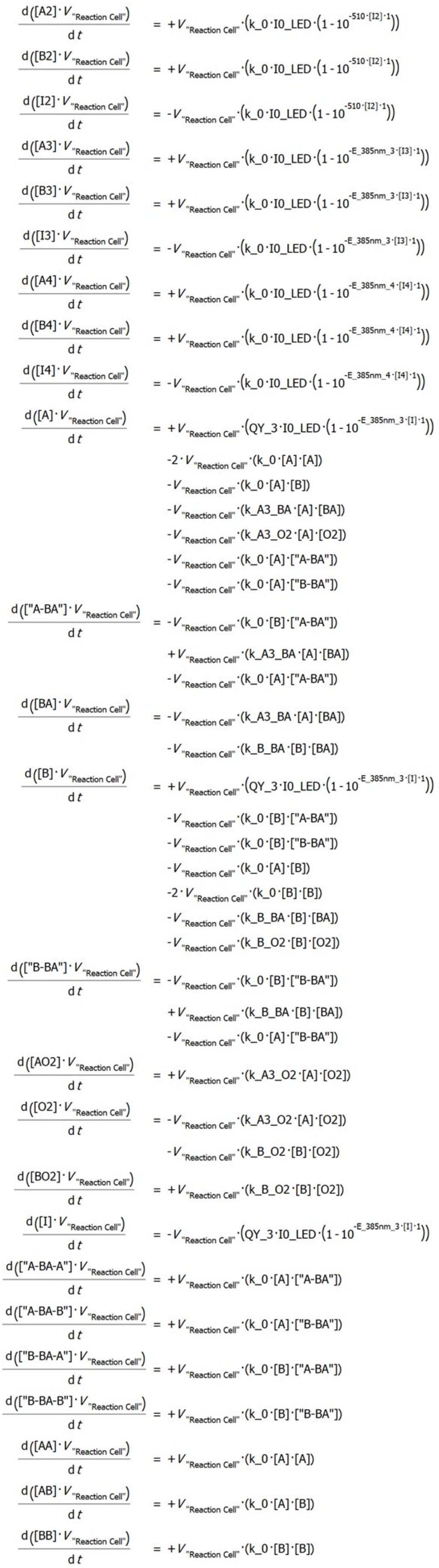

$$\frac{d([A2]\cdot V_{\text{"Reaction Cell"}})}{d t} = +V_{\text{"Reaction Cell"}}\cdot(\text{k\_0}\cdot\text{I0\_LED}\cdot(1-10^{-510\cdot[I2]\cdot 1}))$$

$$\frac{d([B2]\cdot V_{\text{"Reaction Cell"}})}{d t} = +V_{\text{"Reaction Cell"}}\cdot(\text{k\_0}\cdot\text{I0\_LED}\cdot(1-10^{-510\cdot[I2]\cdot 1}))$$

$$\frac{d([I2]\cdot V_{\text{"Reaction Cell"}})}{d t} = -V_{\text{"Reaction Cell"}}\cdot(\text{k\_0}\cdot\text{I0\_LED}\cdot(1-10^{-510\cdot[I2]\cdot 1}))$$

$$\frac{d([A3]\cdot V_{\text{"Reaction Cell"}})}{d t} = +V_{\text{"Reaction Cell"}}\cdot(\text{k\_0}\cdot\text{I0\_LED}\cdot(1-10^{-\text{E\_385nm\_3}\cdot[I3]\cdot 1}))$$

$$\frac{d([B3]\cdot V_{\text{"Reaction Cell"}})}{d t} = +V_{\text{"Reaction Cell"}}\cdot(\text{k\_0}\cdot\text{I0\_LED}\cdot(1-10^{-\text{E\_385nm\_3}\cdot[I3]\cdot 1}))$$

$$\frac{d([I3]\cdot V_{\text{"Reaction Cell"}})}{d t} = -V_{\text{"Reaction Cell"}}\cdot(\text{k\_0}\cdot\text{I0\_LED}\cdot(1-10^{-\text{E\_385nm\_3}\cdot[I3]\cdot 1}))$$

$$\frac{d([A4]\cdot V_{\text{"Reaction Cell"}})}{d t} = +V_{\text{"Reaction Cell"}}\cdot(\text{k\_0}\cdot\text{I0\_LED}\cdot(1-10^{-\text{E\_385nm\_4}\cdot[I4]\cdot 1}))$$

$$\frac{d([B4]\cdot V_{\text{"Reaction Cell"}})}{d t} = +V_{\text{"Reaction Cell"}}\cdot(\text{k\_0}\cdot\text{I0\_LED}\cdot(1-10^{-\text{E\_385nm\_4}\cdot[I4]\cdot 1}))$$

$$\frac{d([I4]\cdot V_{\text{"Reaction Cell"}})}{d t} = -V_{\text{"Reaction Cell"}}\cdot(\text{k\_0}\cdot\text{I0\_LED}\cdot(1-10^{-\text{E\_385nm\_4}\cdot[I4]\cdot 1}))$$

$$\begin{aligned}\frac{d([A]\cdot V_{\text{"Reaction Cell"}})}{d t} = {} & +V_{\text{"Reaction Cell"}}\cdot(\text{QY\_3}\cdot\text{I0\_LED}\cdot(1-10^{-\text{E\_385nm\_3}\cdot[I]\cdot 1}))\\ & -2\cdot V_{\text{"Reaction Cell"}}\cdot(\text{k\_0}\cdot[A]\cdot[A])\\ & -V_{\text{"Reaction Cell"}}\cdot(\text{k\_0}\cdot[A]\cdot[B])\\ & -V_{\text{"Reaction Cell"}}\cdot(\text{k\_A3\_BA}\cdot[A]\cdot[BA])\\ & -V_{\text{"Reaction Cell"}}\cdot(\text{k\_A3\_O2}\cdot[A]\cdot[O2])\\ & -V_{\text{"Reaction Cell"}}\cdot(\text{k\_0}\cdot[A]\cdot[\text{"A-BA"}])\\ & -V_{\text{"Reaction Cell"}}\cdot(\text{k\_0}\cdot[A]\cdot[\text{"B-BA"}])\end{aligned}$$

$$\begin{aligned}\frac{d([\text{"A-BA"}]\cdot V_{\text{"Reaction Cell"}})}{d t} = {} & -V_{\text{"Reaction Cell"}}\cdot(\text{k\_0}\cdot[B]\cdot[\text{"A-BA"}])\\ & +V_{\text{"Reaction Cell"}}\cdot(\text{k\_A3\_BA}\cdot[A]\cdot[BA])\\ & -V_{\text{"Reaction Cell"}}\cdot(\text{k\_0}\cdot[A]\cdot[\text{"A-BA"}])\end{aligned}$$

$$\begin{aligned}\frac{d([BA]\cdot V_{\text{"Reaction Cell"}})}{d t} = {} & -V_{\text{"Reaction Cell"}}\cdot(\text{k\_A3\_BA}\cdot[A]\cdot[BA])\\ & -V_{\text{"Reaction Cell"}}\cdot(\text{k\_B\_BA}\cdot[B]\cdot[BA])\end{aligned}$$

$$\begin{aligned}\frac{d([B]\cdot V_{\text{"Reaction Cell"}})}{d t} = {} & +V_{\text{"Reaction Cell"}}\cdot(\text{QY\_3}\cdot\text{I0\_LED}\cdot(1-10^{-\text{E\_385nm\_3}\cdot[I]\cdot 1}))\\ & -V_{\text{"Reaction Cell"}}\cdot(\text{k\_0}\cdot[B]\cdot[\text{"A-BA"}])\\ & -V_{\text{"Reaction Cell"}}\cdot(\text{k\_0}\cdot[B]\cdot[\text{"B-BA"}])\\ & -V_{\text{"Reaction Cell"}}\cdot(\text{k\_0}\cdot[A]\cdot[B])\\ & -2\cdot V_{\text{"Reaction Cell"}}\cdot(\text{k\_0}\cdot[B]\cdot[B])\\ & -V_{\text{"Reaction Cell"}}\cdot(\text{k\_B\_BA}\cdot[B]\cdot[BA])\\ & -V_{\text{"Reaction Cell"}}\cdot(\text{k\_B\_O2}\cdot[B]\cdot[O2])\end{aligned}$$

$$\begin{aligned}\frac{d([\text{"B-BA"}]\cdot V_{\text{"Reaction Cell"}})}{d t} = {} & -V_{\text{"Reaction Cell"}}\cdot(\text{k\_0}\cdot[B]\cdot[\text{"B-BA"}])\\ & +V_{\text{"Reaction Cell"}}\cdot(\text{k\_B\_BA}\cdot[B]\cdot[BA])\\ & -V_{\text{"Reaction Cell"}}\cdot(\text{k\_0}\cdot[A]\cdot[\text{"B-BA"}])\end{aligned}$$

$$\frac{d([AO2]\cdot V_{\text{"Reaction Cell"}})}{d t} = +V_{\text{"Reaction Cell"}}\cdot(\text{k\_A3\_O2}\cdot[A]\cdot[O2])$$

$$\begin{aligned}\frac{d([O2]\cdot V_{\text{"Reaction Cell"}})}{d t} = {} & -V_{\text{"Reaction Cell"}}\cdot(\text{k\_A3\_O2}\cdot[A]\cdot[O2])\\ & -V_{\text{"Reaction Cell"}}\cdot(\text{k\_B\_O2}\cdot[B]\cdot[O2])\end{aligned}$$

$$\frac{d([BO2]\cdot V_{\text{"Reaction Cell"}})}{d t} = +V_{\text{"Reaction Cell"}}\cdot(\text{k\_B\_O2}\cdot[B]\cdot[O2])$$

$$\frac{d([I]\cdot V_{\text{"Reaction Cell"}})}{d t} = -V_{\text{"Reaction Cell"}}\cdot(\text{QY\_3}\cdot\text{I0\_LED}\cdot(1-10^{-\text{E\_385nm\_3}\cdot[I]\cdot 1}))$$

$$\frac{d([\text{"A-BA-A"}]\cdot V_{\text{"Reaction Cell"}})}{d t} = +V_{\text{"Reaction Cell"}}\cdot(\text{k\_0}\cdot[A]\cdot[\text{"A-BA"}])$$

$$\frac{d([\text{"A-BA-B"}]\cdot V_{\text{"Reaction Cell"}})}{d t} = +V_{\text{"Reaction Cell"}}\cdot(\text{k\_0}\cdot[A]\cdot[\text{"B-BA"}])$$

$$\frac{d([\text{"B-BA-A"}]\cdot V_{\text{"Reaction Cell"}})}{d t} = +V_{\text{"Reaction Cell"}}\cdot(\text{k\_0}\cdot[B]\cdot[\text{"A-BA"}])$$

$$\frac{d([\text{"B-BA-B"}]\cdot V_{\text{"Reaction Cell"}})}{d t} = +V_{\text{"Reaction Cell"}}\cdot(\text{k\_0}\cdot[B]\cdot[\text{"B-BA"}])$$

$$\frac{d([AA]\cdot V_{\text{"Reaction Cell"}})}{d t} = +V_{\text{"Reaction Cell"}}\cdot(\text{k\_0}\cdot[A]\cdot[A])$$

$$\frac{d([AB]\cdot V_{\text{"Reaction Cell"}})}{d t} = +V_{\text{"Reaction Cell"}}\cdot(\text{k\_0}\cdot[A]\cdot[B])$$

$$\frac{d([BB]\cdot V_{\text{"Reaction Cell"}})}{d t} = +V_{\text{"Reaction Cell"}}\cdot(\text{k\_0}\cdot[B]\cdot[B])$$

Figure S20. Screenshot of the differential equations solved by the program.

6. Simulations Considering Standard Deviations of Experimental Data

Figures S21-S23 display simulations of the initiation reaction of photoinitiator **3** in presence of oxygen, taking into account standard errors of the experimental values for quantum yields (Figure S21), extinction coefficients (Figure S22) and rate constants (Figure S23). The simulations have been performed assuming deviations in the experimental values of plus or minus 20 %.

Variations of the quantum yield and extinction coefficient influence the radical generation rate and thus the time scale of the initiation process. An increase of the quantum yield or extinction coefficient leads faster initiation, while a decrease has the opposite effect (see Figures S21 and S22). On the other hand, variations of the monomer addition rate constants influence the concentration ratio of addition radicals (**A(3)-M•** and **B(3)-M•**) to peroxyl radicals (**A(3)-OO•** and **B(3)-OO•**, see Figure S23). This effect is particularly visible in case of the benzoyl radical **B(3)•**. Increasing the monomer addition rate constant by 20% leads to a higher amount of the addition radical **B(3)-M•**, while reducing the formation of the peroxyl radical **B(3)-OO•** (see the main text for further discussions).

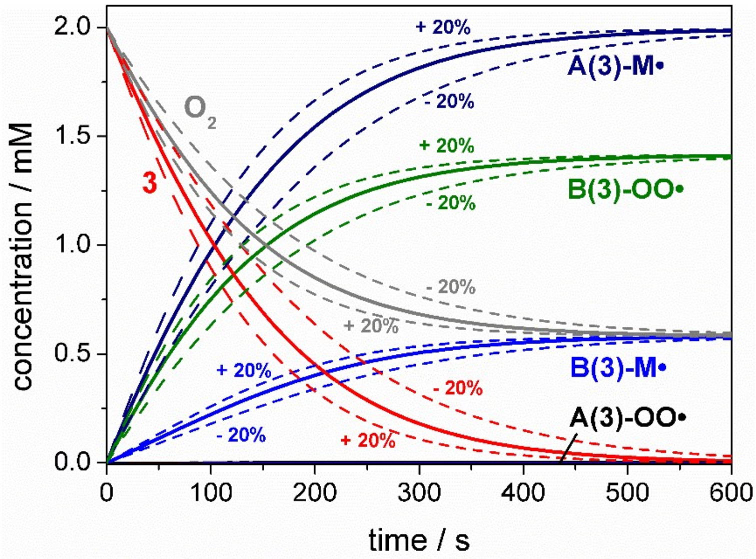

Figure S21. Simulation of the initiation reaction (radical generation followed by monomer addition) for compound **3** in bulk butyl acrylate at 385 nm (I_0 = 2x10^{-5} mol L^{-1}s^{-1}). Solid lines correspond to the following parameters: Φ = 0.83, ε_{385} = 255 L mol^{-1} cm^{-1}, $k_{add,\mathbf{A(3)\bullet}}$ = 2.6 x 10^{8} L mol^{-1} s^{-1}, $k_{add,\mathbf{B(3)\bullet}}$ = 2.7 x 10^{5} L mol^{-1} s^{-1}. The dashed lines show the outcome of the simulations for variations of the experimental quantum yield Φ of plus or minus 20 % (while leaving ε_{385}, $k_{add,A(3)\bullet}$ and $k_{add,B(3)\bullet}$ unchanged).

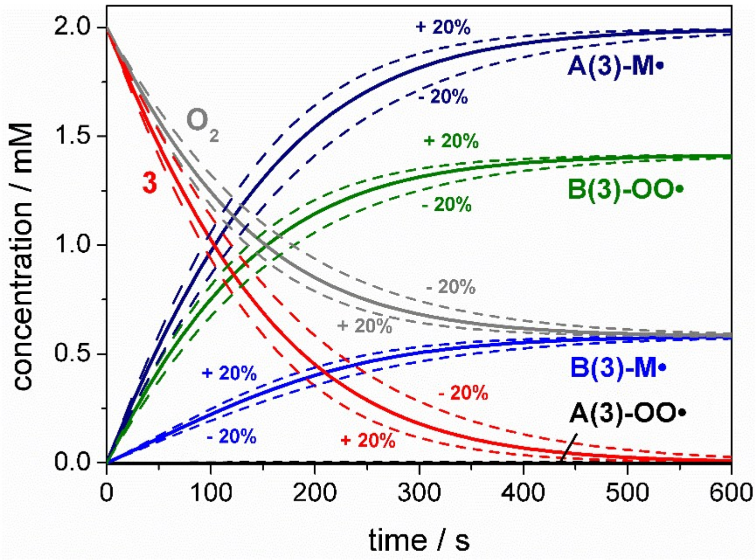

Figure S22. Simulation of the initiation reaction (radical generation followed by monomer addition) for compound **3** in bulk butyl acrylate at 385 nm (I_0 = 2x10^{-5} mol L^{-1}s^{-1}). Solid lines correspond to the following parameters: Φ = 0.83, ε_{385} = 255 L mol^{-1} cm^{-1}, $k_{add,\mathbf{A(3)\bullet}}$ = 2.6 x 10^{8} L mol^{-1} s^{-1}, $k_{add,\mathbf{B(3)\bullet}}$ = 2.7 x 10^{5} L mol^{-1} s^{-1}. The dashed lines show the outcome of the simulations for variations of the experimental extinction coefficient of plus or minus 20 % (while leaving Φ, $k_{add,A(3)\bullet}$ and $k_{add,B(3)\bullet}$ unchanged).

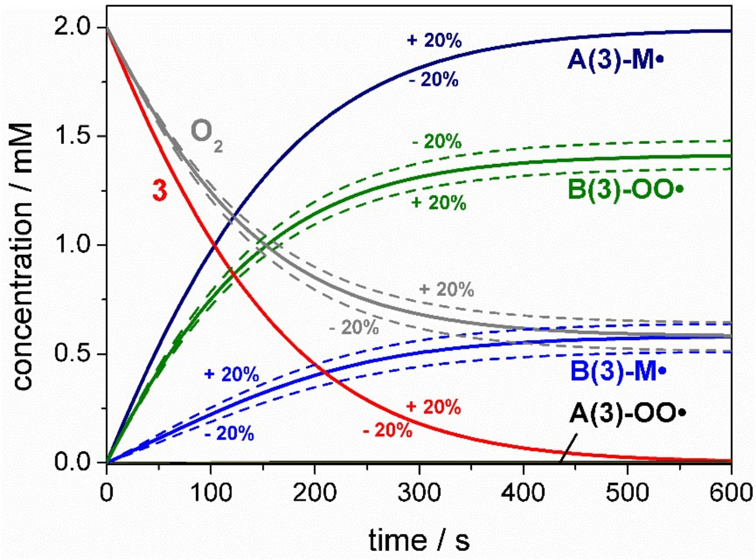

Figure S23. Simulation of the initiation reaction (radical generation followed by monomer addition) for compound **3** in bulk butyl acrylate at 385 nm (I_0 = 2x10^{-5} mol L^{-1}s^{-1}). Solid lines correspond to the following parameters: Φ = 0.83, ε_{385} = 255 L mol^{-1} cm^{-1}, $k_{add,\mathbf{A(3)\bullet}}$ = 2.6 x 10^{8} L mol^{-1} s^{-1}, $k_{add,\mathbf{B(3)\bullet}}$ = 2.7 x 10^{5} L mol^{-1} s^{-1}. The dashed lines show the outcome of the simulations for variations of the experimental monomer addition rate constants of plus or minus 20 % (while leaving Φ and ε_{385} unchanged).